Table 1 Gravimetric and hemodynamic data of WT and SMP30-KO mice

	Control		Ang II	
	WT	SMP30-KO	WT	SMP30-KO
Gravimetric data				
BW, g	26.7 ± 1.1	27.8 ± 1.6	25.6 ± 1.5	27.2 ± 2.2
HW/TL, mg/mm	6.1 ± 0.6	6.5 ± 0.5	7.5 ± 0.6**	8.4 ± 1.0**,†
LVW/TL, mg/mm	4.2 ± 0.5	4.6 ± 0.3	5.7 ± 0.5**	6.7 ± 0.9**,††
Telemetry blood pressure				
HR, b.p.m.	612 ± 48	627 ± 50	593 ± 24	607 ± 65
SBP, mmHg	115.5 ± 12.4	114.8 ± 10.8	140.8 ± 8.6**	144.1 ± 13.7**
DBP, mmHg	85.1 ± 9.4	89.9 ± 9.6	129.4 ± 7.0**	128.6 ± 10.6**
MAP, mmHg	97.8 ± 11.6	99.9 ± 10.4	119.0 ± 6.2**	115.2 ± 9.7**
Echocardiography				
LVEDD, mm	3.77 ± 0.37	3.77 ± 0.38	3.68 ± 0.31	4.26 ± 0.21**,††
LVESD, mm	2.52 ± 0.32	2.42 ± 0.42	2.52 ± 0.35	3.12 ± 0.33**,††
FS, %	33.2 ± 4.4	33.7 ± 4.1	31.8 ± 4.7	25.9 ± 5.2**,††
Catheterization				
LVEDP, mmHg	5.2 ± 1.6	6.0 ± 1.7	9.8 ± 1.0*	11.7 ± 3.0**
max dP/dt, mmHg/s	11 556 ± 850	10 977 ± 940	11 675 ± 999	7303 ± 1107**,††
min dP/dt, mmHg/s	8140 ± 668	8247 ± 384	7582 ± 1408	4804 ± 1897*,†
Tau, ms	4.8 ± 2.0	4.3 ± 0.3	6.3 ± 1.9**	8.3 ± 1.9**

Data are presented as mean ± SD from 10 to 15 mice in each group.
BW, body weight; HW, heart weight; LVW, left ventricular weight; TL, tibial length; HR, heart rate; SBP, systolic blood pressure; DBP, diastolic blood pressure; MAP, mean arterial pressure; LVEDD, left ventricular end-diastolic dimension; LVESD, left ventricular end-systolic dimension; FS, fractional shortening; LVEDP, left ventricular end-diastolic pressure; max and min dP/dt, maximal and minimal rates of left ventricular pressure development, respectively; Tau, time constant of left ventricular isovolumic relaxation.
*$P < 0.05$ and **$P < 0.01$ vs. control in the same strain mice; †$P < 0.05$ and ††$P < 0.01$ vs. Ang II-infused WT mice.

described previously in other organs.[4] Cardiac SMP30 was significantly decreased by 40% at 12-month-old WT mice compared with 3-month-old WT mice ($P < 0.05$, *Figure 1B*). Additionally, cardiac expression of SMP30 was significantly decreased by 50% after Ang II infusion for 14 days in 3-month-old WT mice, suggesting that the expression of SMP30 may alter in cardiovascular diseases ($P < 0.05$, *Figure 1C*).

3.3 Effect of SMP30 deficiency on Ang II-induced cardiac hypertrophy and fibrosis

As shown in *Table 1*, heart weight (HW) and left ventricular weight (LVW) corrected by the tibial length (TL) were similar between control WT mice and SMP30-KO mice. After Ang II infusion, the ratios of HW to TL and LVW to TL were significantly higher in SMP30-KO mice than in WT mice ($P < 0.05$ and $P < 0.01$, respectively), although the blood pressure was similarly elevated in both Ang II-infused WT mice and SMP30-KO mice by telemetry blood pressure monitoring (*Table 1*).

Histological examination showed that Ang II-infused SMP30-KO mice had substantial left ventricular hypertrophy with left ventricular dilatation compared with Ang II-infused WT mice, which suggested eccentric hypertrophy in Ang II-infused SMP30-KO mice compared with concentric hypertrophy in Ang II-infused WT mice (*Figure 2A*, top). The cardiomyocyte cross-sectional area was significantly larger in Ang II-infused SMP30-KO mice than in Ang II-infused WT mice (399 ± 17 vs. 372 ± 11 μm^2, $P < 0.01$, *Figure 2A*, middle and *B*). Additionally, *ex vivo* analysis demonstrated that cell width, length, and surface area of isolated cardiomyocytes were significantly greater in SMP30-KO mice than in WT mice after Ang II stimulation (Supplementary material online, *Figure S1*). The degree of cardiac fibrosis was significantly higher in Ang II-infused SMP30-KO mice than in Ang II-infused WT mice (6.4 ± 0.8 vs. 7.5 ± 0.7%, $P < 0.01$, *Figure 2A*, bottom and *C*). These data revealed that the deficiency of SMP30 exacerbates Ang II-induced cardiac hypertrophy and fibrosis, independently of blood pressure.

3.4 Effect of SMP30 deficiency on Ang II-induced cardiac dysfunction

As shown in *Table 1*, there were no differences in cardiac function between WT mice and SMP30-KO mice under basal conditions. Echocardiography showed that left ventricular end-diastolic and end-systolic dimensions were enlarged and fractional shortening was reduced in SMP30-KO mice compared with WT mice at 14 days after Ang II infusion ($P < 0.01$, *Table 1* and Supplementary material online, *Table S1* and *Figure S2*, top). The left ventricular mass was greater in Ang II-infused SMP30-KO mice than in Ang II-infused WT mice, which was concordant with the histological findings ($P < 0.01$). Ang II-infused SMP30-KO mice had significantly higher peak E velocity, *E/A*, and *E/E'* compared with Ang II-infused WT mice (Supplementary material online, *Table S1* and *Figure S2*, middle and bottom). The mitral inflow showed the restrictive pattern in Ang II-infused SMP30-KO mice in contrast to the relaxation abnormality pattern or the pseudo-normalization pattern in Ang II-infused WT mice. These echocardiographic data revealed that left ventricular systolic and diastolic functions were remarkably depressed in SMP30-KO mice compared with WT mice after Ang II infusion.

Haemodynamic assessment by cardiac catheterization showed that max dP/dt and min dP/dt were significantly lower in SMP30-KO mice than in WT mice after Ang II infusion ($P < 0.01$ and $P < 0.05$,

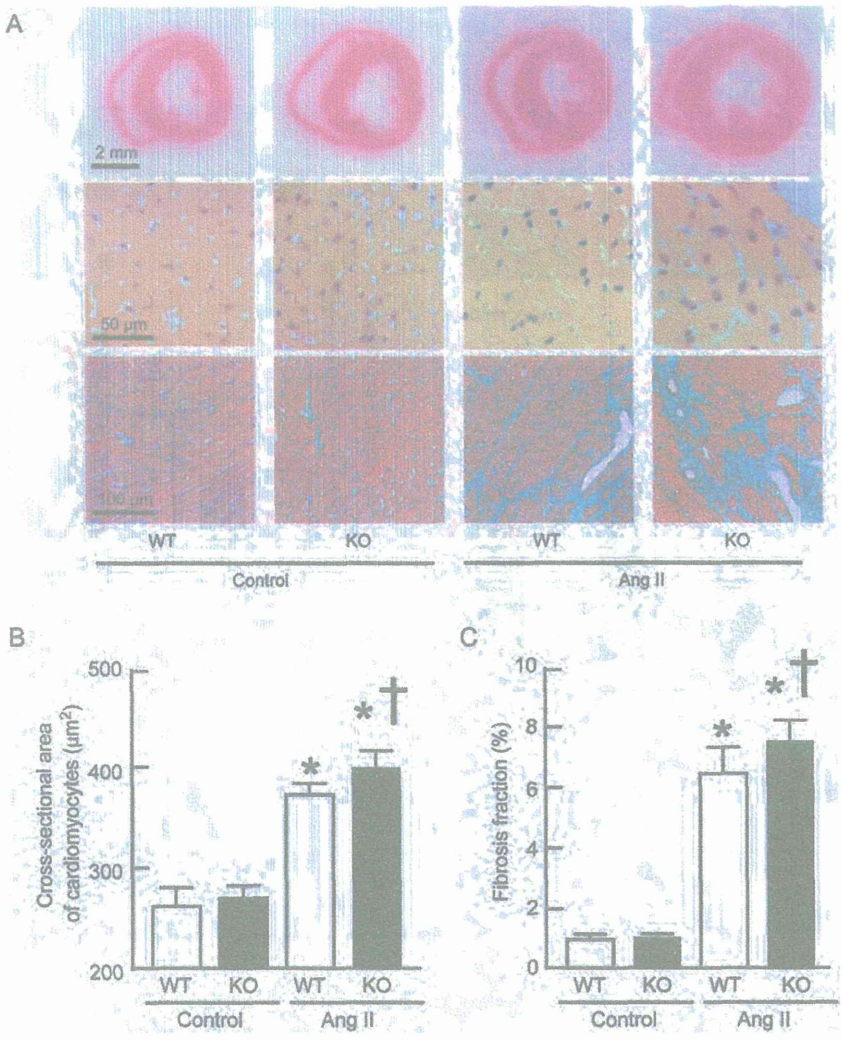

Figure 2 Cardiac hypertrophy and fibrosis in WT and SMP30-KO mice after Ang II infusion. (*A*) Representative images of light micrographs of hearts from WT and SMP30-KO mice with and without Ang II infusion (top). Haematoxylin and eosin staining of myocardial cross-sections (middle). Elastica-Masson staining of myocardial sections (bottom). (*B*) Quantitative analysis of the cross-sectional area of cardiomyocytes from the left ventricle. (*C*) The per cent area of myocardial interstitial fibrosis in the left ventricle. Data are presented as mean ± SD from 6 to 8 mice in each group. $^{*}P < 0.01$ vs. control in the same strain mice; $^{\dagger}P < 0.01$ vs. Ang II-infused WT mice.

respectively), supporting that cardiac systolic and diastolic functions were more severely depressed in SMP30-KO mice (*Table 1*).

3.5 Effect of SMP30 deficiency on Ang II-induced myocardial oxidative stress

We examined myocardial oxidative stress by DHE staining which indicates the O_2levels of living cells because oxidative stress is considered to be one of the important mechanisms of heart failure and cardiac remodelling. Although Ang II infusion dramatically increased the ROS generation in both WT mice and SMP30-KO mice, the ROS generation in Ang II-infused SMP30-KO mice was significantly greater than in Ang II-infused WT mice ($P < 0.01$, *Figure 3A*). In addition, we found that the level of superoxide generation was significantly decreased in Ang II-infused WT mice with apocynin treatment, compared with that of Ang II-infused WT mice without apocynin treatment ($P < 0.01$, *Figure 3A*). As well as WT mice, SMP30-KO mice revealed that Ang II-induced superoxide generation was significantly down-regulated by apocynin treatment ($P < 0.01$, *Figure 3A*).

To investigate the involvement of NADPH oxidase in Ang II-induced ROS generation, we examined the expression of $p67^{phox}$ subunit of NADPH oxidase by western blotting. The expression levels of $p67^{phox}$ were significantly elevated in Ang II-infused SMP30-KO mice compared with Ang II-infused WT mice ($P < 0.01$, *Figure 3B*). These data suggested that the deficiency of SMP30 increased Ang II-induced myocardial oxidative stress via up-regulation of NADPH oxidase.

3.6 Effect of SMP30 deficiency on Ang II-induced apoptosis

As previously demonstrated, SMP30 has anti-apoptotic effects in other organs.[11] We, therefore, checked apoptosis using TUNEL staining

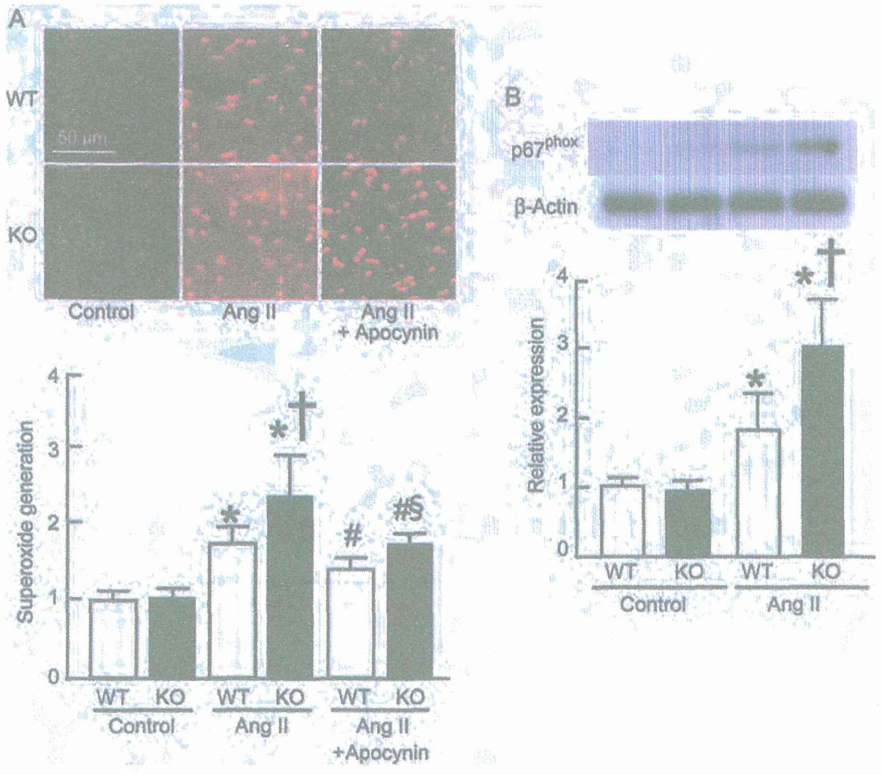

Figure 3 Myocardial oxidative stress in WT and SMP30-KO mice after Ang II infusion. (*A*) Upper panels show representative DHE staining of frozen left ventricular tissues. Lower bar graphs show quantification of superoxide generation. (*B*) Expression of $p67^{phox}$ of NADPH oxidase subunits was analysed by western blotting. Expression levels were expressed relative to those of β-actin. Results are mean ± SD from 6 to 10 mice in each group. $^{*}P < 0.01$ vs. control in the same strain mice; $^{\dagger}P < 0.01$ vs. Ang II-infused WT mice. $^{\#}P < 0.05$ vs. Ang II-infused mice in the same strain; $^{\S}P < 0.05$ vs. Ang II-infused WT mice with apocynin treatment.

(*Figure 4A*). After Ang II infusion, the numbers of TUNEL-positive nuclei including cardiomyocytes and non-cardyomyocytes were increased in both WT and SMP30-KO mice. The numbers of TUNEL-positive nuclei in Ang II-infused SMP30-KO mice were remarkably greater than in Ang II-infused WT mice, as shown in *Figure 4A* ($P < 0.01$).

Then, we examined signalling pathways of Ang II-induced apoptosis in the heart. Caspase-3 is a key mediator of apoptosis, and activation of caspase-3 leads to DNA injury and subsequently apoptotic cell death.[31] The activation of caspase-3 was induced by Ang II infusion in both WT and SMP30-KO mice, and the activation of caspase-3 in Ang II-infused SMP30-KO mice was significantly greater than in Ang II-infused WT mice ($P < 0.01$, *Figure 4B*). After Ang II infusion, Bax expression which functions as pro-apoptotic protein was increased, whereas the expression of anti-apoptotic protein Bcl-2 was decreased in both genotypes of mice. The ratio of Bax to Bcl-2 was significantly higher in Ang II-infused SMP30-KO mice than in Ang II-infused WT mice ($P < 0.01$, *Figure 4C*). Furthermore, we examined the involvement of SAPK/JNK which has a crucial role in cell apoptosis as one main subgroup of the mitogen-activated protein kinase family.[32] Phosphorylation activity of SAPK/JNK in Ang II-infused SMP30-KO mice was significantly increased compared with Ang II-infused WT mice ($P < 0.01$, *Figure 4D*). These findings demonstrated that SMP30 deficiency exacerbates Ang II-induced apoptosis through these signalling pathways.

3.7 Expression of senescence markers in SMP30-KO mice after Ang II infusion

Senescent cells can be identified by the expression of enzymatic SA-β-gal activity in left ventricular tissues (*Figure 5A*). SA β-gal activity was induced by Ang II stimulation. The numbers of SA β-gal-positive cells were significantly greater in Ang II-infused SMP30-KO mice than in Ang II-infused WT mice (1.7 ± 0.8 vs. $0.6 \pm 0.5/mm^3$, $P < 0.01$) as demonstrated in *Figure 5A*.

To evaluate the gene expression of cell cycle inhibitor to confirm senescence of cardiomyocytes, we analysed mRNA expression of p21 gene by RT–PCR (*Figure 5B*). Following Ang II infusion, the expression levels of p21 mRNA were increased in both WT mice and SMP30-KO mice. Compared with Ang II-infused WT mice, Ang II-infused SMP30-KO mice showed a significant increase in p21 expression ($P < 0.01$). These results indicate that deficiency of SMP30 induced cellular senescence after Ang II infusion by the p21-dependent pathway.

4. Discussion

Previous studies have shown that SMP30 acts as an anti-ageing factor, and SMP30 prevents oxidative stress and apoptosis in the liver, lungs, and brain.[11,13,14] However, the role of SMP30 in the heart has not

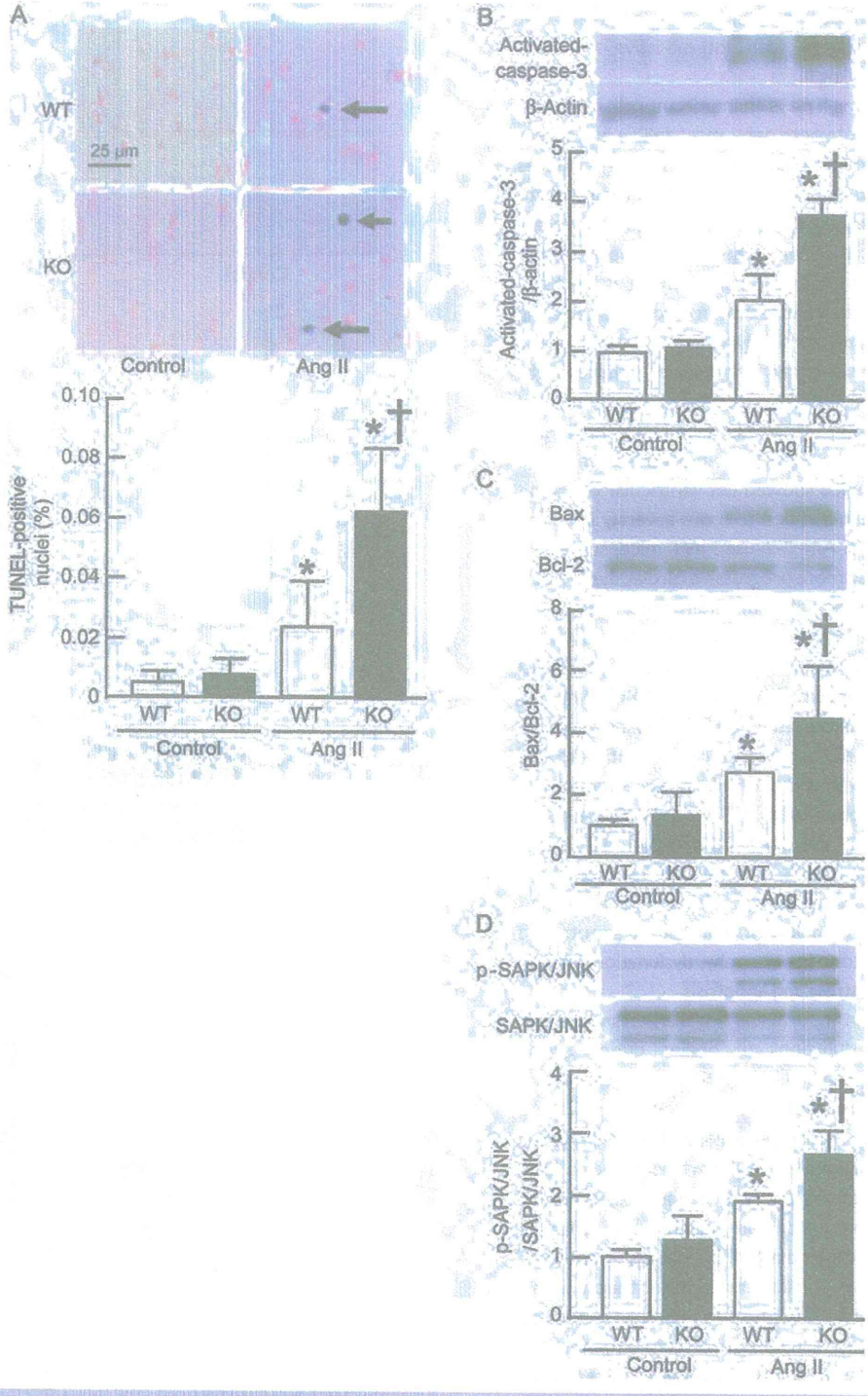

Figure 4 Apoptosis and apoptotic signalling pathways in WT and SMP30-KO mice after Ang II infusion. (*A*) Upper panels show representative images of TUNEL staining of left ventricular tissue sections. Lower bar graph shows the per cent of TUNEL-positive nuclei. (*B*) Activation of caspase-3 was examined by western blotting with anti-activated-caspase-3 antibody using myocardial samples. Expression levels of activated-caspase-3 were normalized by β-actin. (*C*) Expressions of Bax and Bcl-2 were analysed by western blotting. The Bax to Bcl-2 ratio was calculated and presented in the bar graph. (*D*) Phosphorylation activity of SAPK/JNK. Expressions of phosphorylated and total SAPK/JNK were analysed by western blotting. Relative expression levels of phosphorylated SAPK/JNK (P-SAPK/JNK) were expressed in relation to those of SAPK/JNK. Results are mean ± SD from 6 to 10 mice in each group. *$P < 0.01$ vs. control in the same strain mice; †$P < 0.01$ vs. Ang II-infused WT mice.

been investigated. In this study, we demonstrated the first evidence that deficiency of SMP30 exacerbates Ang II-induced cardiac hypertrophy, dysfunction, and adverse remodelling. Our results revealed that SMP30 has a cardio-protective role with anti-oxidative and anti-apoptotic effects in response to Ang II.

It has been well known that Ang II plays an important role in the development of pathological cardiac hypertrophy, remodelling, and subsequent heart failure.[33] Subcutaneous chronic infusion of Ang II induces cardiac hypertrophy and fibrosis with hypertension.[18,34] Ang II also stimulates NADPH oxidase to produce ROS,[35] and consequent myocardial oxidative stress is associated with the development of left ventricular remodelling and heart failure.[36] Furthermore, it has been considered that apoptosis plays an adverse role in cardiac remodelling and contributes to progressive myocardial dysfunction[37] and that Ang II exaggerates apoptotic responses in cardiomyocytes.[38] Interestingly, we observed that deficiency of SMP30 exacerbates Ang II-induced cardiac hypertrophy and fibrosis in SMP30-KO mice (*Table 1*, *Figure 2*, and Supplementary material online, *Figure S1*). Moreover, we found that Ang II-infused SMP30-KO mice showed left ventricular dilatation and depressed systolic function in addition to more severely impaired diastolic function compared with Ang II-infused WT mice, suggesting that the absence of SMP30 caused more progressive cardiac dysfunction and remodelling (*Table 1* and Supplementary material online, *Table S1* and *Figure S2*). These remarkable changes were independent of Ang II-induced hypertension because increased systemic blood pressure of SMP30-KO mice was similar to that of WT mice (*Table 1*). SMP30-KO mice had much more elevated NADPH oxidase-generated ROS by Ang II stimulation (*Figure 3*). In addition, SMP30-KO mice were more susceptible to Ang II-induced apoptosis associated with activation of caspase-3, increase in Bax, decrease in Bcl-2, and phosphorylation of SAPK/JNK (*Figure 4*). Although we were unable to show the direct observation of TUNEL-positive cardiomyocyte nuclei, apoptosis of non-cardiomyocytes plays an important role in Ang II-induced cardiac remodelling and dysfunction as previously reported.[39] These data indicate that SMP30 has a protective role against Ang II-associated cardiac hypertrophy, dysfunction, and remodelling by inhibiting oxidative stress and apoptosis.

SMP30 has been proposed as an important ageing marker, and the lack of SMP30 causes various dysfunctions of organs during ageing process.[11,13–15] Concerning the vitamin C biosynthesis pathway, similar to humans, SMP30-KO mice cannot synthesize vitamin C and SMP30-KO mice may mimic the human physiology closer than other rodents.[40] The potent anti-ageing and anti-oxidative actions of a low-calorie diet effectively suppressed the age-related down-regulation of SMP30, indicating that SMP30 expression was influenced by oxidative stress.[41] These previous reports suggest that SMP30 expression accounts for the age-associated deterioration of cellular function and the enhanced susceptibility to harmful stimuli in aged tissues. On the other hand, very few reports demonstrated cellular senescence of cardiomyocytes *in vivo*.[42,43] We demonstrated that Ang II could increase senescent cells detected by SA β-gal activity *in vivo*. Importantly, Ang II-induced cellular senescence was accompanied with markedly elevated p21 gene expression. SMP30-KO mice showed significantly increased SA β-gal-positive cells with elevated expression of p21 gene by Ang II stimulation, indicating that SMP30 inhibits premature cellular senescence through the signalling pathway of p21 in response to Ang II (*Figure 5*).

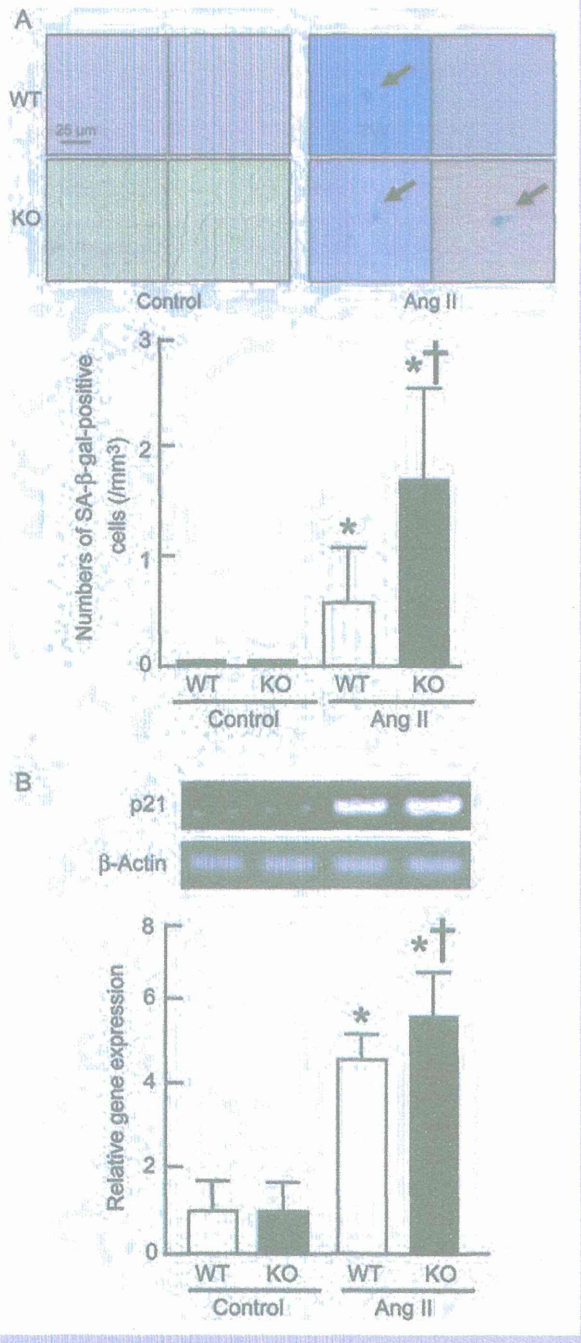

Figure 5 Senescence markers in hearts of WT and SMP30-KO mice after Ang II infusion. (*A*) Senescent cells were detected by SA β-gal staining of left ventricular tissue sections, and the numbers of SA β-gal-positive cells were counted. (*B*) The mRNA expression levels of p21 gene were analysed by RT–PCR. Expression levels of p21 gene were normalized by β-actin. Results are mean ± SD from 6 to 8 mice in each group. *$P < 0.01$ vs. control in the same strain mice; †$P < 0.01$ vs. Ang II-infused WT mice.

There were no differences between WT mice and SMP30-KO mice under basal conditions at 12- to 16-week-old, but we observed that 12-month-old SMP30-KO mice showed exaggerated left ventricular hypertrophy, diastolic dysfunction, and myocardial fibrosis compared with 12-month-old WT mice (Supplementary material online, *Table S2*). One central role of SMP30 in the heart is considered to be the suppressive effect of ROS generation by inhibiting NADPH oxidase activation, as demonstrated in the present study (*Figure 3*). The suppressive role of SMP30 in oxidative stress contributes to the reduction of senescent marker expressions, suggesting that SMP30 prevents myocardial dysfunction from various stresses such as Ang II stimulation and ageing (Supplementary material online, *Figure S3*). Since detailed mechanisms have not been fully clarified, we should evaluate the cellular compartment specific effects of SMP30 in the future study.

5. Conclusions

In summary, deficiency of SMP30 adversely modifies Ang II-induced cardiac hypertrophy and remodelling through increase in oxidative stress and progression of apoptosis. These data provide that SMP30 has a protective role in cardiac remodelling and up-regulation of SMP30 could be a therapeutic target for treatment of heart failure.

Supplementary material

Supplementary material is available at *Cardiovascular Research* online.

Acknowledgements

We thank Ms. Emiko Kaneda for the excellent technical assistance.

Conflict of interest: none declared.

Funding

This study was supported in part by a grant-in-aid for Scientific Research (No. 24591100, Y.T.) from the Japan Society for the Promotion of Science.

References

1. Lakatta EG, Levy D. Arterial and cardiac aging: major shareholders in cardiovascular disease enterprises: part II: the aging heart in health: links to heart disease. *Circulation* 2003;**107**:346–354.
2. Lakatta EG. Arterial and cardiac aging: major shareholders in cardiovascular disease enterprises: part III: cellular and molecular clues to heart and arterial aging. *Circulation* 2003;**107**:490–497.
3. Wang M, Zhang J, Walker SJ, Dworakowski R, Lakatta EG, Shah AM. Involvement of NADPH oxidase in age-associated cardiac remodeling. *J Mol Cell Cardiol* 2010;**48**: 765–772.
4. Fujita T, Uchida K, Maruyama N. Purification of senescence marker protein-30 (SMP30) and its androgen-independent decrease with age in the rat liver. *Biochim Biophys Acta* 1992;**1116**:122–128.
5. Fujita T, Mandel JL, Shirasawa T, Hino O, Shirai T, Maruyama N. Isolation of cDNA clone encoding human homologue of senescence marker protein-30 (SMP30) and its location on the X chromosome. *Biochim Biophys Acta* 1995;**1263**:249–252.
6. Arun P, Aleti V, Parikh K, Manne V, Chilukuri N. Senescence marker protein 30 (SMP30) expression in eukaryotic cells: existence of multiple species and membrane localization. *PLoS ONE* 2011;**6**:e16545.
7. Shimokawa N, Yamaguchi M. Molecular cloning and sequencing of the cDNA coding for a calcium-binding protein regucalcin from rat liver. *FEBS Lett* 1993;**327**:251–255.
8. Son TG, Kim SJ, Kim K, Kim MS, Chung HY, Lee J. Cytoprotective roles of senescence marker protein 30 against intracellular calcium elevation and oxidative stress. *Arch Pharm Res* 2008;**31**:872–877.
9. Little JS, Broomfield CA, Fox-Talbot MK., Boucher LJ, MacIver B, Lenz DE. Partial characterization of an enzyme that hydrolyzes sarin, soman, tabun, and diisopropyl phosphorofluoridate (DFP). *Biochem Pharmacol* 1989;**38**:23–29.
10. Kondo Y, Inai Y, Sato Y, Handa S, Kubo S, Shimokado K *et al.* Senescence marker protein 30 functions as gluconolactonase in L-ascorbic acid biosynthesis, and its knockout mice are prone to scurvy. *Proc Natl Acad Sci USA* 2006;**103**:5723–5728.
11. Ishigami A, Fujita T, Handa S, Shirasawa T, Koseki H, Kitamura T *et al.* Senescence marker protein-30 knockout mouse liver is highly susceptible to tumor necrosis factor-alpha- and Fas-mediated apoptosis. *Am J Pathol* 2002;**161**:1273–1281.
12. Ishigami A, Kondo Y, Nanba R, Ohsawa T, Handa S, Kubo S *et al.* SMP30 deficiency in mice causes an accumulation of neutral lipids and phospholipids in the liver and shortens the life span. *Biochem Biophys Res Commun* 2004;**315**:575–580.
13. Son TG, Zou Y, Jung KJ, Yu BP, Ishigami A, Maruyama N *et al.* SMP30 deficiency causes increased oxidative stress in brain. *Mech Ageing Dev* 2006;**127**:451–457.
14. Sato T, Seyama K, Sato Y, Mori H, Souma S, Akiyoshi T *et al.* Senescence marker protein-30 protects mice lungs from oxidative stress, aging, and smoking. *Am J Respir Crit Care Med* 2006;**174**:530–537.
15. Yumura W, Imasawa T, Suganuma S, Ishigami A, Handa S, Kubo S *et al.* Accelerated tubular cell senescence in SMP30 knockout mice. *Histol Histopathol* 2006;**21**:1151–1156.
16. Hasegawa G, Yamasaki M, Kadono M, Tanaka M, Asano M, Senmaru T *et al.* Senescence marker protein-30/gluconolactonase deletion worsens glucose tolerance through impairment of acute insulin secretion. *Endocrinology* 2010;**151**:529–536.
17. Xue B, Pamidimukkala J, Lubahn DB, Hay M. Estrogen receptor-alpha mediates estrogen protection from angiotensin II-induced hypertension in conscious female mice. *Am J Physiol Heart Circ Physiol* 2007;**292**:H1770–H1776.
18. Kobayashi A, Ishikawa K, Matsumoto H, Kimura S, Kamiyama Y, Maruyama Y. Synergetic antioxidant and vasodilatory action of carbon monoxide in angiotensin II-induced cardiac hypertrophy. *Hypertension* 2007;**50**:1040–1048.
19. Tsao CS, Leung PY, Young M. Effect of dietary ascorbic acid intake on tissue vitamin C in mice. *J Nutr* 1987;**117**:291–297.
20. Carlson SH, Wyss JM. Long-term telemetric recording of arterial pressure and heart rate in mice fed basal and high NaCl diets. *Hypertension* 2000;**35**:E1–E5.
21. Du J, Liu J, Feng HZ, Hossain MM, Gobara N, Zhang C *et al.* Impaired relaxation is the main manifestation in transgenic mice expressing a restrictive cardiomyopathy mutation, R193H, in cardiac TnI. *Am J Physiol Heart Circ Physiol* 2008;**294**:H2604–H2613.
22. Wilson RM, De Silva DS, Sato K, Izumiya Y, Sam F. Effects of fixed-dose isosorbide dinitrate/hydralazine on diastolic function and exercise capacity in hypertension-induced diastolic heart failure. *Hypertension* 2009;**54**:583–590.
23. Kitahara T, Takeishi Y, Harada M, Niizeki T, Suzuki S, Sasaki T *et al.* High-mobility group box 1 restores cardiac function after myocardial infarction in transgenic mice. *Cardiovasc Res* 2008;**80**:40–46.
24. Arimoto T, Takeishi Y, Takahashi H, Shishido T, Niizeki T, Koyama Y *et al.* Cardiac-specific overexpression of diacylglycerol kinase zeta prevents Gq protein-coupled receptor agonist-induced cardiac hypertrophy in transgenic mice. *Circulation* 2006; **113**:60–66.
25. Takimoto E, Champion HC, Li M, Ren S, Rodriguez ER, Tavazzi B *et al.* Oxidant stress from nitric oxide synthase-3 uncoupling stimulates cardiac pathologic remodeling from chronic pressure load. *J Clin Invest* 2005;**115**:1221–1231.
26. Machii H, Saitoh S, Kaneshiro T, Takeishi Y. Aging impairs myocardium-induced dilation in coronary arterioles: role of hydrogen peroxide and angiotensin. *Mech Ageing Dev* 2010; **131**:710–717.
27. Matsushima S, Kinugawa S, Yokota T, Inoue N, Ohta Y, Hamaguchi S *et al.* Increased myocardial NAD(P)H oxidase-derived superoxide causes the exacerbation of postinfarct heart failure in type 2 diabetes. *Am J Physiol Heart Circ Physiol* 2009;**297**:H409–H416.
28. Nozaki N, Shishido T, Takeishi Y, Kubota I. Modulation of doxorubicin-induced cardiac dysfunction in toll-like receptor-2-knockout mice. *Circulation* 2004;**110**:2869–2874.
29. Dimri GP, Lee X, Basile G, Acosta M, Scott G, Roskelley C *et al.* A biomarker that identifies senescent human cells in culture and in aging skin *in vivo*. *Proc Natl Acad Sci USA* 1995;**92**:9363–9367.
30. Camelliti P, Borg TK, Kohl P. Structural and functional characterisation of cardiac fibroblasts. *Cardiovasc Res* 2005;**65**:40–51.
31. Yue TL, Wang C, Romanic AM, Kikly K, Keller P, DeWolf WE Jr *et al.* Staurosporine-induced apoptosis in cardiomyocytes: a potential role of caspase-3. *J Mol Cell Cardiol* 1998;**30**:495–507.
32. Aoki H, Kang PM, Hampe J, Yoshimura K, Noma T, Matsuzaki M *et al.* Direct activation of mitochondrial apoptosis machinery by c-Jun N-terminal kinase in adult cardiac myocytes. *J Biol Chem* 2002;**277**:10244–10250.
33. Weber KT, Brilla CG. Pathological hypertrophy and cardiac interstitium. Fibrosis and renin-angiotensin-aldosterone system. *Circulation* 1991;**83**:1849–1865.
34. Izumiya Y, Kim S, Izumi Y, Yoshida K, Yoshiyama M, Matsuzawa A *et al.* Apoptosis signal-regulating kinase 1 plays a pivotal role in angiotensin II-induced cardiac hypertrophy and remodeling. *Circ Res* 2003;**93**:874–883.
35. Mollnau H, Wendt M, Szocs K, Lassegue B, Schulz E, Oelze M *et al.* Effects of angiotensin II infusion on the expression and function of NAD(P)H oxidase and components of nitric oxide/cGMP signaling. *Circ Res* 2002;**90**:E58–E65.
36. Giordano FJ. Oxygen, oxidative stress, hypoxia, and heart failure. *J Clin Invest* 2005; **115**:500–508.
37. Olivetti G, Abbi R, Quaini F, Kajstura J, Cheng W, Nitahara JA *et al.* Apoptosis in the failing human heart. *N Engl J Med* 1997;**336**:1131–1141.

38. Ravassa S, Fortuno MA, Gonzalez A, Lopez B, Zalba G, Fortuno A *et al.* Mechanisms of increased susceptibility to angiotensin II-induced apoptosis in ventricular cardiomyocytes of spontaneously hypertensive rats. *Hypertension* 2000;**36**:1065–1071.
39. Park M, Shen YT, Gaussin V, Heyndrickx GR, Bartunek J, Resuello RR *et al.* Apoptosis predominates in nonmyocytes in heart failure. *Am J Physiol Heart Circ Physiol* 2009;**297**: H785–H791.
40. Yu R, Schellhorn HE. Recent applications of engineered animal antioxidant deficiency models in human nutrition and chronic disease. *J Nutr* 2013;**143**:1–11.
41. Jung KJ, Ishigami A, Maruyama N, Takahashi R, Goto S, Yu BP *et al.* Modulation of gene expression of SMP-30 by LPS and calorie restriction during aging process. *Exp Gerontol* 2004;**39**:1169–1177.
42. Inuzuka Y, Okuda J, Kawashima T, Kato T, Niizuma S, Tamaki Y *et al.* Suppression of phosphoinositide 3-kinase prevents cardiac aging in mice. *Circulation* 2009;**120**:1695–1703.
43. Maejima Y, Adachi S, Ito H, Hirao K, Isobe M. Induction of premature senescence in cardiomyocytes by doxorubicin as a novel mechanism of myocardial damage. *Aging Cell* 2008;**7**:125–136.

EDITORIAL COMMENTARY

Electrical vagal stimulation and cardioprotection

Kenneth R. Laurita, PhD,* Masamichi Hirose, MD, PhD†

*From the *Heart & Vascular Research Center, MetroHealth Campus, Case Western Reserve University, Cleveland, Ohio, and †Department of Molecular and Cellular Pharmacology, Iwate Medical University, School of Pharmaceutical Sciences, Iwate, Japan.*

When you think of increased vagal tone and its effect on heart rhythm, what comes to mind first is how it slows heart rate and causes atrial fibrillation (AF) with ease, even in the presence of a normal substrate. Paradoxically, it has also been shown that low-level (LL) vagus nerve stimulation (VNS) can decrease AF.[1,2] Clinical[3] and experimental studies[4] have demonstrated that VNS associated with a decrease in heart rate (HR) can also benefit ventricular function. However, much less is known about LL-VNS, when changes in HR are small. This is what, in part, motivated the study by Shinlapawittayatorn et al[5] reported in this issue of Heart*Rhythm,* which focuses on the ventricular benefits of LL-VNS during ischemia reperfusion (I/R).

Main findings

Shinlapawittayatorn et al[5] report several important findings related to the benefits of LL-VNS during I/R. In vivo experiments were performed using swine that underwent left anterior descending artery occlusion (60 minutes), followed by reperfusion (120 minutes). LL-VNS was performed throughout by stimulating the left cervical vagus at a strength that had little to no affect on HR. It is important to note that continuous and intermittent LL-VNS were evaluated. The authors report that LL-VNS during I/R attenuated infarct size, improved ventricular function, and caused a rather dramatic reduction in ventricular tachycardia/ventricular fibrillation (VT/VF) episodes. The functional benefits of VNS have been shown previously,[3,6] but what is interesting from the present study is that similar benefits are reported during LL-VNS in the absence of any significant change in HR. Finally, what might be most interesting to readers is that VT/VF episodes were markedly reduced. Spinal cord stimulation, which can increase vagal tone and decrease sympathetic tone, was shown to reduce ventricular arrhythmias in canines with myocardial infarction.[7] Moreover, Vanoli et al[4] showed that VNS provided significant protection against VF in an animal model of acute myocardial ischemia. Even though HR reduction is often associated with ventricular benefits, in the study by Vanoli et al,[4] protection from VF also was observed during constant atrial pacing, suggesting that reduced HR is not a requirement.

What is the mechanism of reduced VT/VF?

From an electrophysiologic point of view, one of the more interesting questions raised in the study by Shinlapawittayatorn et al[5] is how LL-VNS decreased VT/VF episodes. Like the study by Vanoli et al,[4] reduced HR is not necessary to explain the reduction of arrhythmia vulnerability. VT/VF episodes could be related to the occurrence of premature ventricular complexes (PVCs) (triggers), which, for the most part, was similar. However, it is interesting that with intermittent VNS (with or without atropine), VT/VF during reperfusion did not mirror PVC occurrence. Thus, LL-VNS may be modifying the electrophysiologic substrate in several ways in addition to suppressing triggers (PVCs). VNS can also antagonize sympathetic outflow to the heart, which has well-known proarrhythmic action. Such may be the mechanism whereby LL-VNS can suppress AF. For example, Shen et al[8] showed that left-sided LL-VNS can suppress stellate ganglion nerve activity (LSGNA) immediately and cause neuronal remodeling over time.

There is some evidence that suppression of LSGNA can improve ventricular function[9] and, possibly, suppress ventricular arrhythmias. Gao et al[10] showed that pretreatment with electro-acupuncture can protect against ventricular arrhythmias during I/R due to inhibition of beta-adrenergic signaling and the L-type calcium channel. In addition, reduced LSGNA may attenuate reverse mode activation of the Na^+/Ca^{2+} exchanger, which has been associated with stimulation of $alpha_1$-adrenergic receptors during I/R.[11] These results suggest that reduced LSGNA may prevent arrhythmias during I/R that are due to calcium overload. There are several other possibilities whereby LL-VNS may modify the electrophysiologic substrate, such as that related to reduced reactive oxygen species (ROS)[12,13] (as shown in the present study) or even by preserving myocardial connexin43 expression.[14] Unfortunately, these mechanistic pathways are all speculative, and there is no clear reason

Address reprint requests and correspondence: Dr. Kenneth R. Laurita, Heart & Vascular Research Center, MetroHealth Campus of Case Western Reserve University, Rammelkamp, 6th Floor, 2500 MetroHealth Dr, Cleveland, OH 44109-1998. E-mail address: klaurita@metrohealth.org.

http://dx.doi.org/10.1016/j.hrthm.2013.08.033

why LL-VNS decreased VT/VF, as observed in the present study. Of course, one simple explanation is that LL-VNS modified the structural substrate by reducing infarct size, which, from wavelength theory, could explain the reduction of VT/VF episodes observed.

What caused the decrease in infarct size?

Shinlapawittayatorn et al[5] report a significant decrease in infarct size with LL-VNS. This is paralleled by an attenuation of mitochondrial ROS, depolarization, and swelling, all of which may reduce apoptosis. Others have shown that VNS can inhibit the release of proapoptotic signals associated with mitochondria dysfunction and, thus, attenuate cardiac injury.[15] Alternatively, Calvillo et al[16] described the antiinflammatory and antiapoptotic properties of the nicotinic pathway as the primary mechanism underlying VNS-induced decrease in infarct size during cardiac I/R. However, this action by the nicotinic pathway was partial. Therefore, the present study provides some interesting insight regarding the role of muscarinic (ie, atropine sensitive) LL-VNS activation in the reduction of infarct size during I/R. Finally, infarct size during I/R can be reduced by inhibition of inflammasome activation in cardiac fibroblasts.[17] Given that ROS can activate inflammasomes (eg, NLRP3),[18] then this may also be a mechanism by which LL-VNS reduced infarct size, as observed in the present study.

Clinical implications

Independent of the potential causal relationships discussed, the findings reported by Shinlapawittayatorn et al[5] have important clinical implications. First, the results of this study suggest that LL-VNS may be an effective therapeutic strategy for preventing the loss of ventricular function and increased VF episodes that are associated with I/R. Given that VNS is a safe and efficacious treatment of neurologic disorders (eg, seizure prevention and control), utilization for cardioprotection may be emerging. Second, the benefits are achieved by stimulating the left cervical vagus rather than the right. This is ideal because of the greater number of cardiac efferent fibers from the right vagus nerve, including innervation of the sinoatrial node. Accordingly, altered heart rate and other possible undesirable consequences can be avoided. Third, intermittent LL-VNS performed better than continuous. Continuous LL-VNS may have caused tachyphylaxis, which sometimes can result from a marked reduction in the amount of acetylcholine. Alternatively, this can be explained by desensitization of receptors available to acetylcholine, which occurs in response to saturation.[19] In contrast, intermittent LL-VNS seems to not exhibit tachyphylaxis.

Summary

You may be scratching your head and be a bit disappointed if you crave a mechanistic understanding of why LL-VNS decreased VT/VF episodes. However, this does not diminish the potential clinical implications of the findings reported by Shinlapawittayatorn et al.[5] LL-VNS may be an important treatment strategy to prevent VF/VT episodes and preserve ventricular function during acute ischemia. If this can be achieved without undesirable consequences associated with VNS, then this approach could have a significant impact on patients with ischemic heart disease.

References

1. Shen MJ, Shinohara T, Park HW, et al. Continuous low-level vagus nerve stimulation reduces stellate ganglion nerve activity and paroxysmal atrial tachyarrhythmias in ambulatory canines. Circulation 2011;123:2204–2212.
2. Li S, Scherlag BJ, Yu L, et al. Low-level vagosympathetic stimulation: a paradox and potential new modality for the treatment of focal atrial fibrillation. Circ Arrhythm Electrophysiol 2009;2:645–651.
3. De Ferrari GM, Crijns HJ, Borggrefe M, et al. Chronic vagus nerve stimulation: a new and promising therapeutic approach for chronic heart failure. Eur Heart J 2011;32:847–855.
4. Vanoli E, De Ferrari GM, Stramba-Badiale M, Hull SS Jr, Foreman RD, Schwartz PJ. Vagal stimulation and prevention of sudden death in conscious dogs with a healed myocardial infarction. Circ Res 1991;68:1471–1481.
5. Shinlapawittayatorn K, Chinda K, Palee S, et al. Low-amplitude, left vagus nerve stimulation significantly attenuates ventricular dysfunction and infarct size through prevention of mitochondrial dysfunction during acute ischemia-reperfusion injury. Heart Rhythm 2013;10:1700–1707.
6. Li M, Zheng C, Sato T, Kawada T, Sugimachi M, Sunagawa K. Vagal nerve stimulation markedly improves long-term survival after chronic heart failure in rats. Circulation 2004;109:120–124.
7. Lopshire JC, Zhou X, Dusa C, et al. Spinal cord stimulation improves ventricular function and reduces ventricular arrhythmias in a canine postinfarction heart failure model. Circulation 2009;120:286–294.
8. Shen MJ, Hao-Che C, Park HW, et al. Low-level vagus nerve stimulation upregulates small conductance calcium-activated potassium channels in the stellate ganglion. Heart Rhythm 2013;10:910–915.
9. Lobato EB, Kern KB, Paige GB, Brown M, Sulek CA. Differential effects of right versus left stellate ganglion block on left ventricular function in humans: an echocardiographic analysis. J Clin Anesth 2000;12:315–318.
10. Gao J, Zhang L, Wang Y, et al. Antiarrhythmic effect of acupuncture pretreatment in rats subjected to simulative global ischemia and reperfusion–involvement of adenylate cyclase, protein kinase A, and L-type Ca^{2+} channel. J Physiol Sci 2008;58:389–396.
11. Woodcock EA, Arthur JF, Harrison SN, Gao XM, Du XJ. Reperfusion-induced Ins(1,4,5)P(3) generation and arrhythmogenesis require activation of the Na(+)/Ca(2+) exchanger. J Mol Cell Cardiol 2001;33:1861–1869.
12. Greensmith DJ, Eisner DA, Nirmalan M. The effects of hydrogen peroxide on intracellular calcium handling and contractility in the rat ventricular myocyte. Cell Calcium 2010;48:341–351.
13. Cutler MJ, Plummer BN, Wan X, et al. Aberrant S-nitrosylation mediates calcium-triggered ventricular arrhythmia in the intact heart. Proc Natl Acad Sci USA 2012;109:18186–18191.
14. Ando M, Katare RG, Kakinuma Y, et al. Efferent vagal nerve stimulation protects heart against ischemia-induced arrhythmias by preserving connexin43 protein. Circulation 2005;112:164–170.
15. Lu X, Costantini T, Lopez NE, et al. Vagal nerve stimulation protects cardiac injury by attenuating mitochondrial dysfunction in a murine burn injury model. J Cell Mol Med 2013;17:664–671.
16. Calvillo L, Vanoli E, Andreoli E, et al. Vagal stimulation, through its nicotinic action, limits infarct size and the inflammatory response to myocardial ischemia and reperfusion. J Cardiovasc Pharmacol 2011;58:500–507.
17. Kawaguchi M, Takahashi M, Hata T, et al. Inflammasome activation of cardiac fibroblasts is essential for myocardial ischemia/reperfusion injury. Circulation 2011;123:594–604.
18. Tschopp J, Schroder K. NLRP3 inflammasome activation: the convergence of multiple signalling pathways on ROS production? Nat Rev Immunol 2010;10:210–215.
19. Contrera JG, McLeskey SW, Holopainen I, Xu J, Wojcik WJ. Muscarinic m2 receptors in cerebellar granule cell cultures from rat: mechanism of short-term desensitization. J Pharmacol Exp Ther 1993;265:433–440.

Histochem Cell Biol
DOI 10.1007/s00418-013-1082-0

ORIGINAL PAPER

Effects of protease-activated receptors (PARs) on intracellular calcium dynamics of acinar cells in rat lacrimal glands

Makoto Oikawa · Tomoyuki Saino · Katsura Kimura · Yuki Kamada · Yasunori Tamagawa · Daijiro Kurosaka · Yoh-ichi Satoh

Accepted: 4 February 2013

Abstract Protease-activated receptors (PARs) represent a novel class of seven transmembrane domain G-protein coupled receptors, which are activated by proteolytic cleavage. PARs are present in a variety of cells and have been prominently implicated in the regulation of a number of vital functions. Here, lacrimal gland acinar cell responses to PAR activation were examined, with special reference to intracellular Ca^{2+} concentration ($[Ca^{2+}]_i$) dynamics. In the present study, detection of acinar cell mRNA specific to known PAR subtypes was determined by reverse transcriptase polymerase chain reaction. Only PAR2 mRNA was detected in acinar cells of lacrimal glands. Both trypsin and a PAR2-activating peptide (PAR2-AP), SLIGRL-NH_2, induced an increase in $[Ca^{2+}]_i$ in acinar cells. The removal of extracellular Ca^{2+} and the use of Ca^{2+} channel blockers did not inhibit PAR2-AP-induced $[Ca^{2+}]_i$ increases. Furthermore, U73122 and xestospongin C failed to inhibit PAR2-induced increases in $[Ca^{2+}]_i$. The origin of the calcium influx observed after activated PAR2-induced Ca^{2+} release from intracellular Ca^{2+} stores was also evaluated. The NO donor, GEA 3162, mimicked the effects of PAR2 in activating non-capacitative calcium entry (NCCE). However, both calyculin A (100 nM) and a low concentration of Gd^{3+} (5 μM) did not completely block the PAR2-AP-induced increase in $[Ca^{2+}]_i$. These findings indicated that PAR2 activation resulted primarily in Ca^{2+} mobilization from intracellular Ca^{2+} stores and that PAR2-mediated $[Ca^{2+}]_i$ changes were mainly independent of IP_3. RT-PCR indicated that TRPC 1, 3 and 6, which play a role in CCE and NCCE, are expressed in acinar cells. We suggest that PAR2-AP differentially regulates both NCCE and CCE, predominantly NCCE. Finally, our results suggested that PAR2 may function as a key receptor in calcium-related cell homeostasis under pathophysiological conditions such as tissue injury or inflammation.

Keywords Lacrimal gland · Protease-activated receptors · Intracellular calcium · Confocal microscopy · RT-PCR

M. Oikawa · T. Saino (✉) · Y. Tamagawa · Y. Satoh
Department of Anatomy (Cell Biology),
Iwate Medical University, 2-1-1 Nishitokuda,
Yahaba, Iwate 028-3694, Japan
e-mail: tsaino@iwate-med.ac.jp

K. Kimura (✉) · Y. Kamada · D. Kurosaka
Department of Ophthalmology, School of Medicine,
Iwate Medical University, 19-1 Uchimaru, Morioka,
Iwate 020-8505, Japan
e-mail: kimukatu@iwate-med.ac.jp

Introduction

The lacrimal gland is responsible for secretion of electrolytes, water, proteins and mucins, collectively known as lacrimal gland fluid, into the tear film. The appropriate amount and composition of lacrimal gland fluid is crucial for a healthy, intact ocular surface (Dartt 2009). Regulation of these secretions is under neural control, and activation of the sensory nerves in the cornea and conjunctiva initiates an afferent pathway leading to the central nervous system. This pathway activates an efferent pathway that stimulates parasympathetic and sympathetic nerves, innervating the lacrimal gland (Hodges and Dartt 2003).

Protease-activated receptors (PARs) represent a novel class of seven transmembrane domain G-protein coupled receptors (GPCRs) that are activated by proteolytic cleavage (Déry et al. 1998). Four members of this class of

Published online: 06 March 2013